

Microwave-assisted rapid fabrication of Co_3O_4 nanorods and application to the degradation of phenol

Teh-Long Lai^{a,b}, Yuan-Lung Lai^c, Chia-Chan Lee^a, Youn-Yuen Shu^{b,*}, Chen-Bin Wang^{a,*}

^a Department of Applied Chemistry and Materials Science, Chung Cheng Institute of Technology, National Defense University, Tahsi, Taoyuan 33509, Taiwan ROC

^b Environmental Analysis Laboratory, Department of Chemistry, National Kaohsiung Normal University, Kaohsiung 802, Taiwan ROC

^c Department of Mechanical and Automation Engineering, Da-Yeh University, Changhua 515, Taiwan ROC

Available online 26 November 2007

Abstract

A novel microwave-assisted hydrothermal route for preparation of Co_3O_4 nanorods had been developed. The process contained two steps: first, nanorods of cobalt hydroxide carbonate were obtained from a mixed solution of 50 ml of 0.6 M $\text{Co}(\text{NO}_3)_2 \cdot 6\text{H}_2\text{O}$ and 2.4 g of urea under 500 W microwave irradiated for 3 min. Then, the cobalt hydroxide carbonate nanorods were calcined at 400 °C to fabricate pure cobaltic oxide (Co_3O_4) nanorods. Both nanorods were characterized by X-ray diffraction (XRD), scanning electron microscopy (SEM), thermogravimetry (TG), infrared (IR) and temperature-programmed reduction (TPR). The catalytic activity towards the degradation of phenol over Co_3O_4 nanorods was further studied under continuous bubbling of air through the liquid phase. The results showed that phenol was degraded into harmless products (CO_2 and malonic acid). The mechanism of phenol degradation was also discussed.

© 2007 Elsevier B.V. All rights reserved.

Keywords: Microwave-assisted; Co_3O_4 Nanorods; Degradation of phenol

1. Introduction

Metal oxides are widely used in the field of heterogeneous catalysis. Cobalt oxide is one of the most versatile materials among transition metal oxides [1,2]. Cobaltic oxide (Co_3O_4) with a variety of morphologies, i.e., nanoparticles, nanotubes, nanocubes, nanofiber, and hollow spheres has been reported. A convenient technique to prepare nanocrystalline oxides in very short durations is the microwave-assisted hydrothermal [3,4]. The advantages of the microwave-assisted hydrothermal process over the conventional hydrothermal method are: (a) extremely rapid kinetics of crystallization, (b) very rapid heating to the required temperature and (c) possible formation of new meta-stable phases [5]. Carp et al. [6] choosing a pair ligand-outer sphere ions (such as urea-nitrate ion) direct the synthesis in obtaining fine oxide particles which can prevent the sintering of oxides. Microwave irradiation technology has

already been applied to industry, family, medical science and environmental organic pollution for polycyclic aromatic hydrocarbons (PAHs) [7–9] and polychlorinated biphenyls (PCBs) [10], etc. Due to the properties of internal and volumetric heating (dipole rotation and/or ionic conduction), thermal gradients during microwave processing are avoided, providing a uniform environment for reaction. Therefore, microwave heating has shown higher energy efficiency and reaction rates to shorten reaction times [11]. The use of microwaves as a source of energy is rapidly becoming more economical and convenient. In this study, we report on the fabrication of Co_3O_4 nanorods through the thermal decomposition of cobalt hydroxide carbonate nanorods which were prepared by the microwave-assisted hydrothermal process.

Co_3O_4 is very attractive in the application of oxidation reactions because of the presence of mobile oxygen, i.e., unsupported cobalt oxide is an active catalyst in air pollution control for the abatement of CO [12,13], NO_x [14,15] and organic pollutants from effluent streams [16,17]. Also, cobalt oxide is important in the development of rechargeable batteries [18–20] and the CO sensor [21–23]. From this point of view, we adopt Co_3O_4 nanorods as active components in the current work

* Corresponding authors. Fax: +886 33 892494.

E-mail addresses: shuyy@nknuc.nknu.edu.tw (Y.-Y. Shu), chenbinwang@gmail.com (C.-B. Wang).

and combine microwave irradiation technology to promote the degradation of phenol. Co_3O_4 nanorods might be a good candidate for practical application in the abatement of environmental pollutants.

2. Experimental

2.1. Catalyst preparation and characterization

In order to prepare cobalt hydroxide carbonate nanorods as starting materials, $\text{Co}(\text{NO}_3)_2 \cdot 6\text{H}_2\text{O}$ and urea had been chosen. A mixed solution of 50 ml of 0.6 M $\text{Co}(\text{NO}_3)_2 \cdot 6\text{H}_2\text{O}$ and 2.4 g of urea was irradiated under 500 W (Milston MSD1000) microwave for 3 min. The precipitate was then filtered, washed with deionized distilled water, and dried in an oven at 100 °C for 20 h to obtain the solid sample (assigned as as-prepared). Then, the as-prepared sample was further calcined under air at 400 °C for 3 h to obtain the black species (assigned as C400). The Co_3O_4 nanoparticle was synthesized by the precipitation–oxidation method in an aqueous solution. The detailed preparation procedure was described in a previous paper [24]. Then, the as-prepared sample was further calcined under 400 °C in air for 3 h to obtain the black species (assigned as P400).

X-ray diffraction (XRD) measurements were performed using a MAC Science MXP18 diffractometer with $\text{Cu K}\alpha 1$ radiation ($\lambda = 1.5405 \text{ \AA}$) at 40 kV and 30 mA with a scanning speed in 2θ of 4° min^{-1} . The morphologies and sizes of the samples were observed through a scanning electron microscopy (SEM). The scanning electron microscopy images were taken on a JSM-6330TF SEM operated at 10 kV. Thermal gravimetric analysis (TG/DTG) was carried out using a Seiko SSC5000 TG system. The rate of heating was maintained at $10^\circ \text{C min}^{-1}$ and the mass of the sample was 10 mg. The temperature was raised from room temperature to 800 °C under an air flow with a rate of 100 ml min^{-1} . Reduction behavior of the samples was studied with temperature-programmed reduction (TPR). About 50 mg of the sample was heated in a flow of 10% H_2/N_2 gas mixture at a flow rate of 10 ml min^{-1} . During TPR, the temperature was increased at a $7^\circ \text{C min}^{-1}$ increment from room temperature to 600 °C. The infrared spectra were obtained by a Nicolet 5700 FT-IR spectrometer in the range of 400–2000 cm^{-1} . One milligram of each powder sample was diluted with 200 mg of vacuum-dried IR-grade KBr and subjected to a pressure of 8 tons.

2.2. Degradation of phenol

The microwave-enhanced catalytic degradation (MECD) [25] experiments were carried out in a controllable temperature unit microwave apparatus (CEM Discover, USA) that can program the reaction temperature and time. The system operated at 2450 MHz and worked at 100 W. The temperature can be controlled precisely within $\pm 2^\circ \text{C}$ from the set temperature through the use of an IR sensor. The reaction vessel was a conical flask that was connected to a simple refluxing device. Twenty milliliters of aqueous phenol solution (initial concentration of 200 ppm) was used for each experi-

mental run. Air was bubbled in the solution for 30 min before being added to the catalyst. Then, 40 mg of catalyst was suspended in the solution. The air was continuously bubbled during the runs.

The chromatographic experiments were performed using high performance liquid chromatograph (HPLC) that was equipped with diode array detector and a column oven. A $125 \text{ mm} \times 4 \text{ mm}$ reverse-phase C-18 column (chrompack) was used for separation. The operational parameters were: 20 μl injection volume, 1.0 ml/min flow rate, 270 nm wavelength of UV detector and oven temperature of the column was maintained 25 °C. The compounds were eluted with $\text{CAN}/\text{H}_2\text{O}$ (v/v, 50/50). Qualitative of the degradation intermediates was carried out on an Agilent 1100 Series LC/MS liquid chromatograph–mass spectrometer (LC/MS) system.

3. Results and discussion

3.1. Characterization of the prepared samples

Fig. 1(a) shows the XRD pattern of the as-prepared sample by the microwave-assisted hydrothermal process. It indicates that the sample consisted of a mixed phase of cobalt hydroxide carbonate. All the diffraction peaks can be perfectly indexed to both phases with the orthorhombic cobalt basic carbonate [JCPDS card, no. 48-0083, $\text{Co}(\text{OH})_x(\text{CO}_3)_{0.5-0.11}\text{H}_2\text{O}$] and the monoclinic cobalt hydroxide carbonate [JCPDS card, no. 29-1416, $\text{Co}_2(\text{OH})_2\text{CO}_3$]. After the thermal decomposition of cobalt hydroxide carbonate precursor under 400 °C for 3 h, a single phase of well crystallized Co_3O_4 with the cubic structure (JCPDS card, no. 80-1541, Co_3O_4) was obtained [Fig. 1(b)]. No peaks of other phase have been detected, indicating that the C400 sample is of high purity. The XRD pattern of the P400 is given in Fig. 1(c). All peaks appear similar to the C400 sample that can be indexed as the cubic Co_3O_4 . Comparison the strength of diffraction peaks, the perfect nanorods structure possesses better crystalline than the nanoparticles.

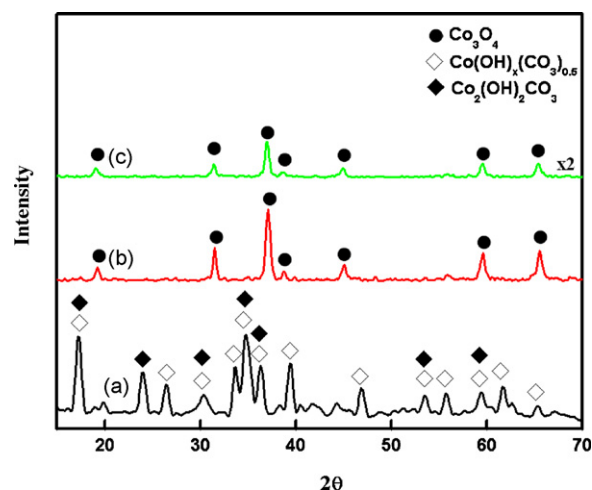


Fig. 1. XRD spectra of: (a) as-prepared; (b) C400; (c) P400.

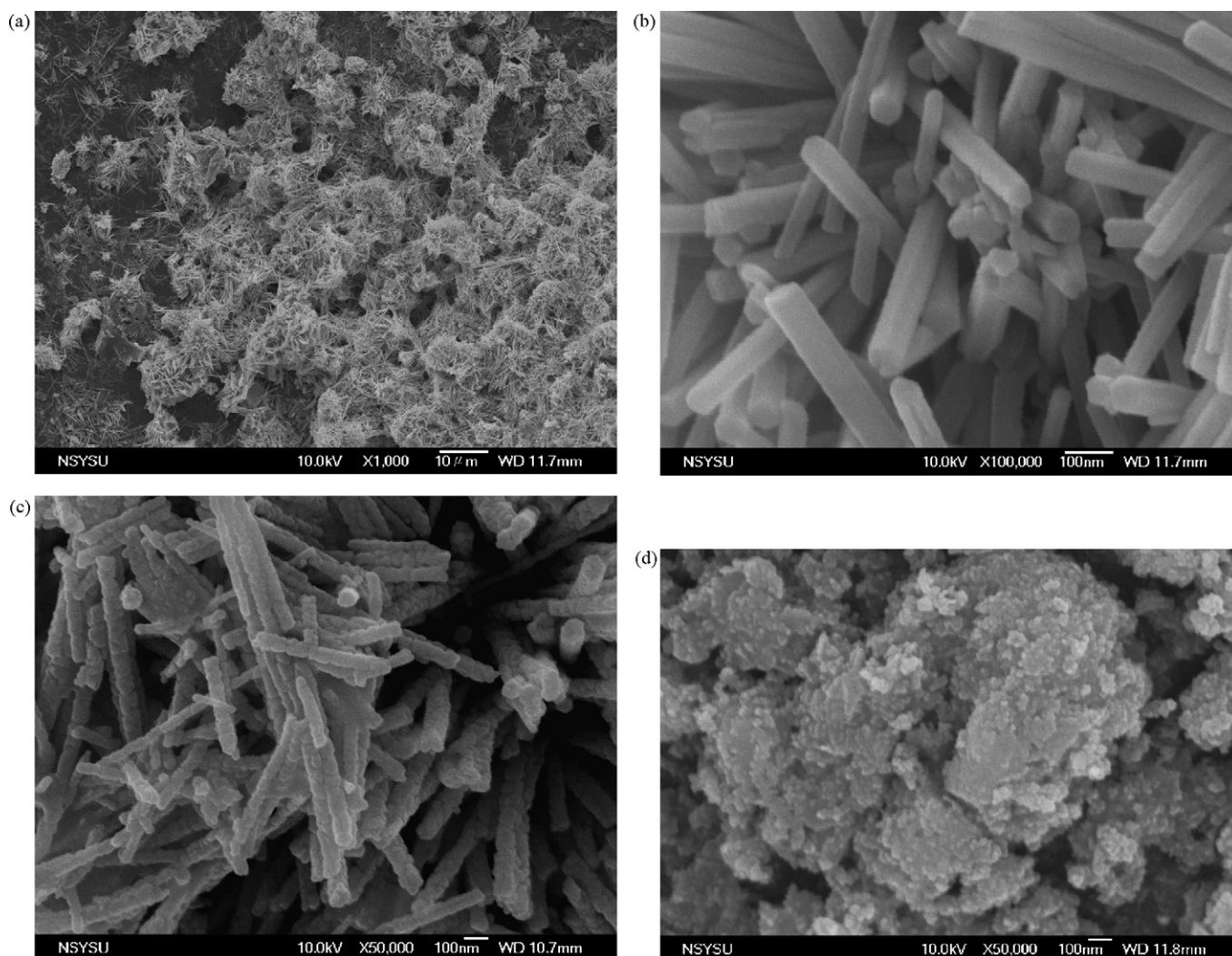


Fig. 2. SEM micrographs of: (a) as-prepared ($\times 1,000$); (b) as-prepared ($\times 100,000$); (c) C400 ($\times 50,000$); (d) P400 ($\times 50,000$).

The SEM images of the mixed phase of cobalt hydroxide carbonate are shown in Fig. 2(a and b). From our observations of the present images, the as-prepared sample is bamboo-like nanorods with a diameter varying from 30 to 60 nm, and a length of hundreds to thousands of nanometers. The morphology [Fig. 2(c)] of the post-thermal decomposition of cobalt hydroxide carbonate product indicates that the C400 sample looks like a series of bead-chains formed by lots of Co_3O_4 nanoparticles interconnection with each other in a definite direction to construct nanorods. Fig. 2(d) shows the SEM image of the P400 sample. It can be seen that the agglomeration of particles is present. Generally, it can be considered that the agglomeration of nanoparticles comes from the interfacial reaction under heat treatment.

Fig. 3 shows the TG/DTG curves for the thermal decomposition of as-prepared sample under air flow (100 ml min^{-1}). The TG curve shows an obvious weight loss (22.5%) around 287°C (according to the DTG curve). Similar weight loss and decomposed temperature of the as-prepared sample are observed from Li et al. [26] group for their synthesized cobalt hydroxide carbonate. Based on the theoretical weight loss of cobalt hydroxide carbonate, the simultaneous removal of hydroxy and

carbonate anions, and followed the oxidation of cobalt ion to form cobaltic oxide occurs according to the following equation which approaches to 24% loss.

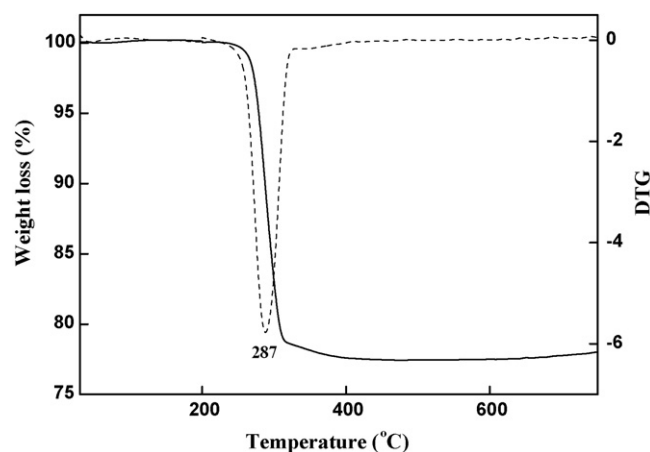
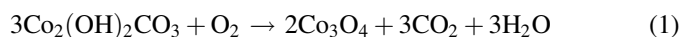


Fig. 3. TG/DTG curves for the thermal decomposition of as-prepared sample under air flow.

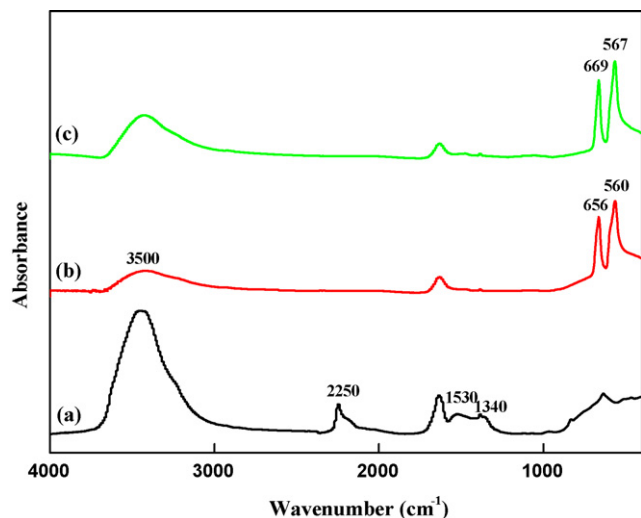


Fig. 4. IR spectra of: (a) as-prepared; (b) C400; (c) P400.

Comparison with the structural analysis of XRD, the result further confirms the compositions of as-prepared and C400 samples.

In order to understand the crystallographic sites occupation and the cationic jumps along the phase transition of cobalt oxides, the IR absorption spectra are measured for cobalt hydroxide carbonate and cobalt oxide. Fig. 4(a) shows the absorption spectra of as-prepared sample. In the spectrum of cobalt hydroxide carbonate nanorods, the prominent band at 1340–1530 cm^{-1} is typical of CO_3^{2-} ions. The peaks at 2250 cm^{-1} is assigned to CO_2 residues. The IR spectrum of cobaltic oxide nanorods [Fig. 4(b)] and nanoparticles [Fig. 4(c)] displays two distinct and sharp bands at 560 (ν_1) and 656 (ν_2) cm^{-1} and 567 (ν_1) and 669 (ν_2) cm^{-1} , respectively, that originated from the stretching vibrations of the metal-oxygen bond [27,28]. The ν_1 band is characteristic of OB_3 (where B denotes the Co^{3+} in the octahedral hole) vibration and the ν_2 band is attributed to the ABO_3 (where A denotes the Co^{2+} in the tetrahedral hole) vibration in the spinal lattice [29]. The broad peak around 3500 cm^{-1} , corresponding to $-\text{OH}$, is also decreased in intensity. This means that the CO_2 and CO_3^{2-} are almost removed while still containing some hydroxyl group that comes from the adsorbed water after calcination at 400 $^\circ\text{C}$.

Fig. 5(a) shows the TPR profile of the as-prepared sample. The reductive signal of cobaltic hydroxide carbonate in TPR shows only one step at 345 $^\circ\text{C}$ according to Eq. (2).

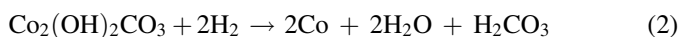


Fig. 5(b) shows the TPR profile of C400 sample. The reductive signal of cobaltic oxide in TPR shows two consecutive steps at 311 and 351 $^\circ\text{C}$. The similar reductive behavior can be observed from the nanoparticles. Fig. 5(c) shows the reductive signal of P400 sample which presents two consecutive steps at 307 and 359 $^\circ\text{C}$. According to our previous reports [30,31], the cobaltic oxide nanorods and nanoparticles are initially reduced to CoO , and then further reduced to Co . Apparently, the following two successive steps are designated

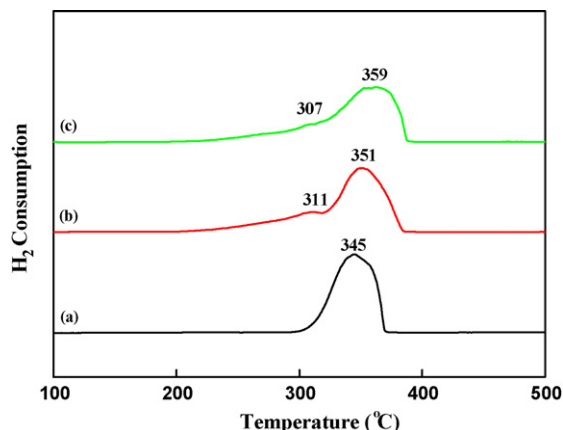


Fig. 5. TPR profiles of: (a) as-prepared; (b) C400; (c) P400.

on raising the temperature:



3.2. Microwave-enhanced catalytic degradation of phenol over Co_3O_4 nanorods

Fig. 6 shows the catalytic activity of MECD for phenol over cobaltic oxide nanorods and nanoparticles under pH 7 and $T = 70$ $^\circ\text{C}$. It can be seen that phenol degradation is 82% within 400 min over cobaltic oxide nanorods and 74% within 400 min over cobaltic oxide nanoparticles. Since the nanorods are constructed by lots of Co_3O_4 nanoparticles to form bead-chains that possess the larger aspect ratio than nanoparticles to absorb microwave, we suggest that the cobaltic oxide nanorods are more sensitive to absorbed microwave to enhance the degradation. In the degradation of the carbon skeleton and total oxidation, Bielanski and Haber [32] proved with EPR that the formation of electrophilic oxygen ions from the adsorbed of oxygen on the p-type oxides (e.g., NiO , CoO , and Co_3O_4) showed high activity in catalytic reactions. According to the

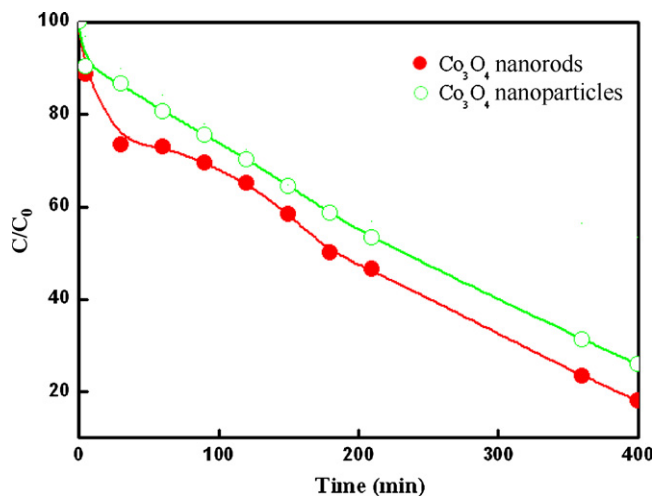


Fig. 6. Conversion profile for phenol MECD over C400 and P400.

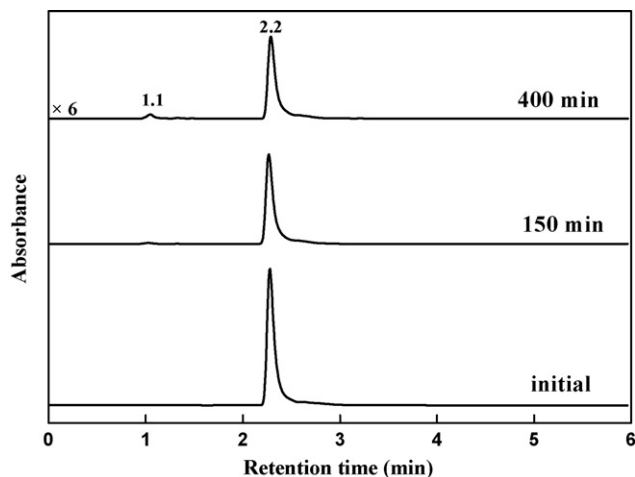


Fig. 7. HPLC spectra of phenol degraded during MECD method over C400 sample under pH 7 and $T = 70\text{ }^{\circ}\text{C}$.

literature describing, we think that under the irradiation of microwave, the electrophilic oxygen ions (O_2^- , O^- and O^{2-} that come from lattice oxygen) on the cobaltic oxides can be donated to participate the degradation of phenol and captured oxygen from air. On the other hand, the higher activity over NiO_x on the degradation of phenol comes from the coupling effect between microwave and active oxygen species on nickel oxide surface [25] that is easier than Co_3O_4 . In order to investigate the intermediate, both the HPLC and LC–MS have been used. Fig. 7 shows the HPLC spectra of phenol degraded during MECD. The peak appears at 2.2 min, which is typical species of phenol. This peak gradually diminishes along with the proceeding of the MECD. Aside from the phenol peak, another small peak appears at 1.1 min that is suggested to be the intermediate. Collection of the intermediate is characterized by LC/MS and shown in Fig. 8. The m/e of 104.4 demonstrates that the intermediate is malonic acid [$\text{CH}_2(\text{CO}_2\text{H})_2$]. Quintanilla et al. [33] studied the catalytic oxidation of phenol over a Fe/AC catalyst and suggested that the malonic acid arose from hydroquinone. Therefore, the identified products of phenol degraded during MECD over cobaltic oxide nanorods are CO_2 (mainly) and malonic acid according to the following reaction pathway.



Fig. 9 shows the reaction pathway for phenol degradation by MECD method over cobaltic oxide nanorods. Air is con-

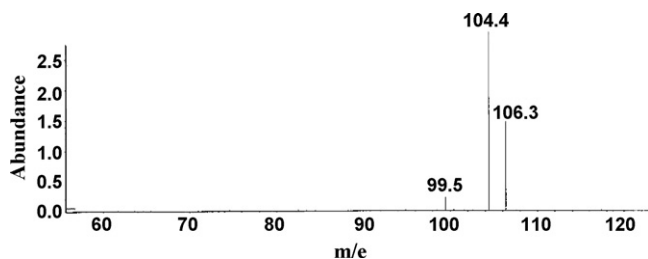


Fig. 8. Mass spectrum of the collected elution from HPLC after 400 min reaction.

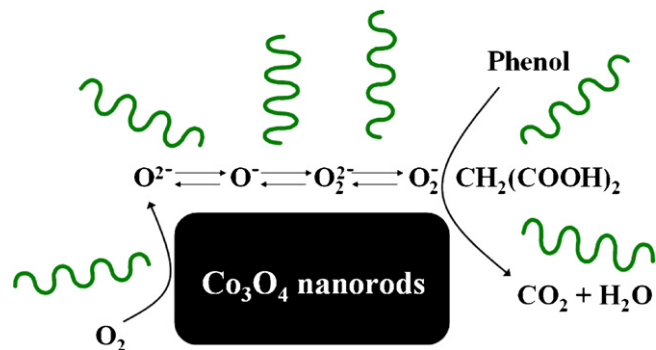


Fig. 9. The reaction pathway for phenol degradation by MECD method over cobaltic oxides.

tinuously bubbled during the runs. In the cyclic route, electrophilic oxygen ions generated from cobaltic oxides can participate in the degradation of phenol under the irradiation of microwave.

4. Conclusion

This study developed a novel and environmentally friendly method for fabricating cobaltic oxide nanorods and application to the degradation of phenol. The following conclusions have been made:

- (1) We successfully synthesized nanorods of cobalt hydroxide carbonate through a rapid microwave-assisted hydrothermal process. Further, the pure Co_3O_4 nanorods were obtained from the calcination of cobalt hydroxide carbonate under $400\text{ }^{\circ}\text{C}$.
- (2) Phenol was degraded into harmless products (CO_2 and malonic acid) by the MECD method under pH 7 and $T = 70\text{ }^{\circ}\text{C}$ over Co_3O_4 nanorods.

Acknowledgements

We are pleased to acknowledge the financial support for this study from the National Science Council of the Republic of China under contract numbers NSC 94-2113-M-014-002 and NSC M95-2113-M-026-001.

References

- [1] H.G. Lin, H.C. Chiu, H.C. Tasi, S.H. Chien, C.B. Wang, Catal. Lett. 88 (2003) 169.
- [2] C.B. Wang, H.G. Lin, C.W. Tang, Catal. Lett. 94 (2004) 69.
- [3] S. Baldassari, S. Komarneni, E. Mariani, C. Villa, Mater. Res. Bull. 40 (2005) 2014.
- [4] X. Liao, J. Zhu, W. Zhong, H.Y. Chen, Mater. Lett. 50 (2001) 341.
- [5] A.V. Murugan, V. Samuel, V. Ravi, Mater. Lett. 60 (2006) 479.
- [6] O. Carp, L. Patron, A. Reller, Mater. Chem. Phys. 101 (2007) 142.
- [7] Y.Y. Shu, T.L. Lai, J. Chromatogr. A 927 (2001) 131.
- [8] Y.Y. Shu, T.L. Lai, H.S. Lin, T.C. Yang, C.P. Chang, Chemosphere 52 (2003) 1667.
- [9] Y.Y. Shu, R.C. Lao, C.H. Chiu, R. Turle, Chemosphere 41 (2000) 1709.
- [10] Y.Y. Shu, S.S. Wang, M. Tardif, Y.P. Huang, J. Chromatogr. A 1008 (2003) 1.

- [11] H.M. Kingston, L.B. Jassie, *Introduction to Microwave Sample Preparation*, American Chemical Society, Washington, 1988, p. 7.
- [12] Y.J. Mergler, J. Hoebink, B.E. Nieuwenhuys, *J. Catal.* 167 (1997) 305.
- [13] J. Jansson, *J. Catal.* 194 (2000) 55.
- [14] H. Hamada, Y. Kintaichi, M. Inaba, M. Tabata, T. Yoshinari, H. Tsuchida, *Catal. Today* 29 (1996) 53.
- [15] D. Pietrogiaconi, S. Tuti, M.C. Campa, V. Indovina, *Appl. Catal. B* 28 (2000) 43.
- [16] E. Garbowski, M. Guenin, M.C. Marion, M. Primet, *Appl. Catal.* 64 (1990) 209.
- [17] A.S.K. Sinha, V. Shankar, *J. Chem. Eng. Biochem. Eng.* 52 (1993) 115.
- [18] F. Lichtenberg, K. Kleinsorgen, *J. Power Sources* 62 (1996) 207.
- [19] E. Antolini, E. Zhecheva, *Mater. Lett.* 35 (1998) 380.
- [20] T.J. Boyle, D. Ingersoll, T.M. Alam, C.J. Tafoya, M.A. Rodriguez, K. Vanheusden, D.H. Dougherty, *Chem. Mater.* 10 (1998) 2770.
- [21] H. Yamaura, J. Tamaki, K. Moriya, N. Miura, N. Yamazoe, *J. Electrochem. Soc.* 144 (1997) L158.
- [22] H. Yamaura, K. Moriya, N. Miura, N. Yamazoe, *Sens. Actuators B* 65 (2000) 39.
- [23] E. Gulari, C. Guldur, S. Srivannavit, S. Osuwan, *Appl. Catal. A* 182 (1999) 147.
- [24] H.G. Lin, H.C. Chiu, H.C. Tsai, S.H. Chien, C.B. Wang, *Catal. Lett.* 94 (2004) 69.
- [25] T.L. Lai, C.C. Lee, K.S. Wu, Y.Y. Shu, C.B. Wang, *Appl. Catal. B* 68 (2006) 147.
- [26] B. Li, Y. Xie, C.Z. Wu, Z.Q. Li, J. Zhang, *Mater. Chem. Phys.* 99 (2006) 479.
- [27] C. Spenser, D. Schroeder, *Phys. Rev. B* 9 (1974) 3658.
- [28] T. Andrushkevich, G. Boreskov, V. Popovskii, L. Pliasova, L. Karakchiev, A. Ostankovitch, *Kinet. Katal.* 6 (1968) 1244.
- [29] St.G. Christoskova, M. Stoyanova, M. Georgieva, D. Mehandjiev, *Mater. Chem. Phys.* 60 (1999) 39.
- [30] C.B. Wang, C.W. Tang, S.J. Gau, S.H. Chien, *Catal. Lett.* 101 (2005) 59.
- [31] C.W. Tang, C.C. Kuo, M.C. Kuo, C.B. Wang, S.H. Chien, *Appl. Catal. A* 309 (2006) 37.
- [32] A. Bielanski, J. Haber, *Catal. Rev. Sci. Eng.* 19 (1979) 1.
- [33] A. Quintanilla, J.A. Casas, A.F. Mohedano, J.J. Rodriguez, *Appl. Catal. B* 67 (2006) 206.